Chinese Chemical Letters 35 (2024) 109303

Contents lists available at ScienceDirect

Chinese Chemical Letters

journal homepage: www.elsevier.com/locate/cclet

A DNA micro-complex containing polyaptamer for exosome separation and wound healing

Jingwen Zhao[a], Jianpu Tang[b], Zhen Cui[b], Limin Liu[a], Dayong Yang[b,*], Chi Yao[b,*]

[a] Department of Gastroenterology and Hepatology, Tianjin Medical University General Hospital, Tianjin Institute of Digestive Disease, Tianjin Key Laboratory of Digestive Diseases, Tianjin 300052, China
[b] Frontiers Science Center for Synthetic Biology, Key Laboratory of Systems Bioengineering (MOE), School of Chemical Engineering and Technology, Tianjin University, Tianjin 300350, China

ARTICLE INFO

Article history:
Received 29 August 2023
Revised 10 November 2023
Accepted 14 November 2023
Available online 21 November 2023

Keywords:
DNA nanotechnology
DNA materials
Aptamer
Exosomes
Wound healing

ABSTRACT

Exosomes (EXOs) have showed great potential in regenerative medicine. The separation of EXOs from complex biological media is essential for the down-stream applications. Herein, we report a deoxyribonucleic acid (DNA)-based micro-complex (DMC) containing polyaptamers, which realized the specific separation of EXOs from cell culture media and the significant promotion of wound healing. The synthesis of DMCs was based on a biomineralization process *via* rolling circle amplification (RCA) under the catalysis of phi29 DNA polymerase. To endow DMCs with the ability to capture EXOs, the DNA template of RCA was integrated with complementary sequence of aptamer that specifically recognized the CD63 proteins on EXOs. The obtained DMCs contained polyaptamers that can specifically capture the EXOs in cell culture media. The EXOs-capturing DMCs were collected by centrifugation, achieving the separation of EXOs. Mesenchymal stem cell (MSC)-derived EXOs (MSC-EXOs) were separated by this DMC-based strategy, and the separated MSC-EXOs significantly enhanced the migration ability of cells. In particular, the significant therapeutic efficacy of the DMCs with MSC-EXOs was verified in full-thickness wound excision mouse models, in which the wounds completely healed in 10 days. We envision that this DMC-based separation strategy can be a promising route to promote the development of EXOs in biomedicine.

Exosomes (EXOs) as a type of extracellular vesicles contain various bioactive molecules, such as ribonucleic acids, proteins and lipids [1,2]. Studies have proven that the EXOs in organisms participate the substance transportation among cells and regulate a series of physiological processes [3,4]. With the development of the biological functions of EXOs, EXOs showed great potential as therapeutic agents for biomedical applications [5–10]. Recently, a series of efficient physical approaches, such as mechanics and electricity [11–14], and chemical therapeutic regents [15,16] had been developed for wound healing. In particular, the mesenchymal stem cell (MSC)-derived EXOs were proven to possess the biological functions of reducing cell apoptosis, alleviating inflammatory response, promoting angiogenesis, and inhibiting fibrosis, which showed great clinical application prospects in wound healing [17–19]. As the prerequisite of down-stream applications, the separation of EXOs from complex biological systems, such as body fluids or culture media, is of great significance [20–22]. However, challenges remain in the separation of EXOs, due to the natural properties of EXOs, including the small sizes (usually 30–150 nm) and the similar densities to the medium. More notably, the structure and biological activity of EXOs are easily damaged by the external stimulation in separation process, such as shear force and medium change. In addition, traditional technologies of EXO separation, such as ultracentrifugation and polymer-based precipitation, usually require a large volume of samples, specialized equipment and complicated operation. Therefore, developing new strategies based on new materials is one of the most promising routes to solve the problems in EXOs separation.

In recent years, deoxyribonucleic acid (DNA) nanotechnology has been utilized in the field of biological separation. For instance, some of the nanotechnologies were based on DNA aptamers, a category of oligonucleotide sequences that can recognize target ligands with high affinity and specificity [23–25]. By integrating the aptamers that can recognize the biomarker on the target cells or cell-derived vesicles, the DNA materials were endowed with the capability to recognize the target cells and cell-derived vesicles [26–28]. Remarkably, rolling circle amplification (RCA) as an efficient enzymatic amplification of DNA has been used to produce the

* Corresponding authors.
E-mail addresses: dayong.yang@tju.edu.cn (D. Yang), chi.yao@tju.edu.cn (C. Yao).

https://doi.org/10.1016/j.cclet.2023.109303
1001-8417/

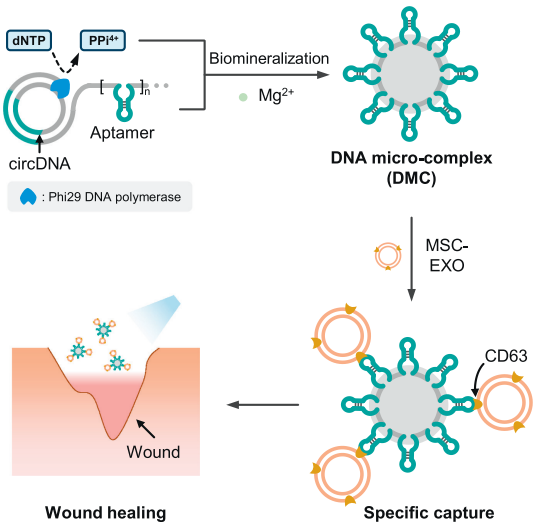

Scheme 1. Schematic illustration of DNA micro-complex (DMC) for exosome (EXO) separation and wound healing. The DMCs were constructed *via* the biomineralization process in rolling circle amplification with the catalysis of phi29 DNA polymerase. The polyvalent aptamers in DMCs specifically captured EXOs by recognizing the CD63 proteins on the membrane. circDNA, circular DNA; dNTP, deoxyribonucleoside triphosphate; PPi^{4+}, pyrophosphate group; MSC, mesenchymal stem cell.

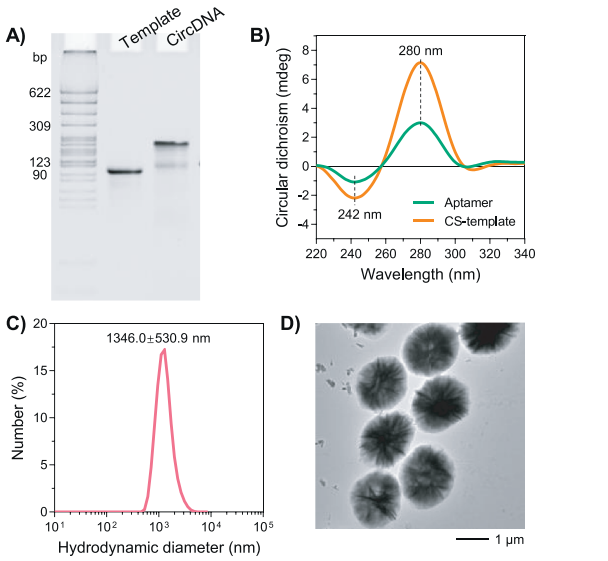

Fig. 1. Synthesis and characterization of DMCs. (A) 12% native polyacrylamide gel electrophoresis to verify the cyclizing of template. (B) Circular dichroism spectra of aptamer and the complementary sequence of linear template (CS-template). (C) Dynamic light scattering assay of DMCs. (D) Transmission electron microscopy image of DMCs.

ultralong single-stranded DNA (ssDNA) with polyvalent aptamers [29,30], which realized the specific separation of MSCs and T lymphocytes [31,32]. It is expected to develop new DNA materials that are designed with the specific polyaptamers towards EXOs, achieving the separation of EXOs from complex biological media.

Biomineralization is a complex and dynamic process that can transform the metal ions in solution into solid minerals under the control of biological organic substances, which have progressed from organically-controlled crystallization to biofunctional material construction, opening up a new route for related research and applications [33]. Herein, we report a biomineralization-based DNA micro-complex (DMC) that contains polyaptamers, realizing the specific separation of MSC-derived EXOs (MSC-EXOs) from cell culture media, and demonstrate the therapeutic effect of the separated EXOs in full-thickness wound excision mouse models.

The DMCs were constructed *via* a biomineralization process in RCA, in which a circular DNA (circDNA) worked as the template to produce a large amount of ssDNA with the tandem repeated sequences complementary to circDNA [34]. In our design, the complementary sequence of an aptamer that specifically recognized the tetraspanin (CD63) on EXO membrane was integrated in the circDNA [35–37]. Upon the catalysis of phi29 DNA polymerase, the ultralong ssDNA with polyvalent aptamers was produced; meanwhile, a large amount of pyrophosphate group (PPi^{4+}) was produced due to the decomposition of deoxyribonucleoside triphosphates. Afterwards, the ultralong ssDNA, PPi^{4+}, and magnesium ion (Mg^{2+}) in the system combined, achieving the construction of DMCs (Scheme 1). The polyvalent aptamers in DMCs can specifically recognize and capture the MSC-EXOs in cell culture media; the separation of EXOs on DMCs was then achieved by centrifugation. By spraying the EXOs-capturing DMCs on the wound region, the viability and migration ability of cells were significantly enhanced, thus promoting the healing rate of wound (Scheme 1).

The circDNA was constructed by two short ssDNA (template and primer, Table S1 in Supporting information) through annealing and enzymatic ligation. The result of 12% native-polyacrylamide gel electrophoresis showed that the movement rate of circDNA was slower than that of linear template (Fig. 1A), which was due to the larger spatial hindrance caused by the more complex structure and higher molecular weight of circDNA, indicating the successful cyclization of the template. To prove the integration of the complementary sequences of aptamer in the template, circular dichroism spectra of both aptamer and the complementary sequence of linear template (CS-template) were measured. As shown in Fig. 1B, the positive Cotton effect peak of CS-template overlapped with that of aptamer at 280 nm, and the negative Cotton effect peak of CS-template overlapped with that of aptamer at 242 nm, indicating the same secondary structure between CS-template and aptamer, demonstrating the integration of the complementary sequences of aptamer in linear template.

RCA was carried out under the catalysis of phi29 DNA polymerase for 6 h, and then the DMCs were obtained by centrifugation. The result of dynamic light scattering showed that average hydrodynamic diameter of DMCs was 1346.0 nm (Fig. 1C). To further verify the successful synthesis of DMCs, the microtopography of DMCs was observed by scanning electron microscopy, which showed that the DMCs were uniform microscale spherical particles (Fig. S1 in Supporting information). In addition, both scanning electron microscopy image and transmission electron microscopy image showed the porous structure of DMCs (Fig. S1 and Fig. 1D), which effectively increased the contact area of DMCs with EXOs due to the high specific surface area, and was beneficial for the separation of EXOs.

The cell culture media used for EXO separation were obtained after culturing MSCs for two days, and then pre-treated by gradient centrifugation to remove impurities, such as cells and cell debris, after which the EXOs were retained in the media due to their similar density to media. The separation process of EXOs included three steps (Fig. 2A): (i) the DMCs were added into the pre-treated media, and the polyvalent aptamers on DMCs selectively recognized and bound with the CD63 proteins on EXOs, achieving the specific capture of EXOs by DMCs; (ii) the mixture was treated by centrifugation, and the DMCs with EXOs were centrifugated to the bottom of tube due to the higher density of DMCs than media; (iii) the supernatant of media was removed, and the DMCs with EXOs (DMC@EXO) were washed and dissolved by phosphate buffered saline (PBS). To test the stability of DMCs in the process of EXO separation, DMCs were incubated in 10% serum at 37 °C. The

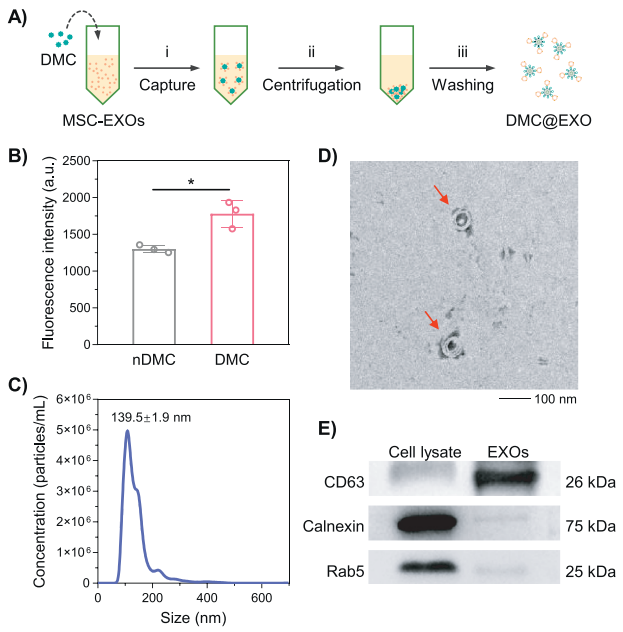

Fig. 2. Separation of MSC-EXOs by DMCs. (A) Schematic illustration of the separation process of MSC-EXOs by DMCs. (B) Statistics of fluorescence intensity of the EXOs captured by nDMCs and DMCs. nDMCs, DMCs without aptamer. Statistical analysis was performed using by two-tailed unpaired *t*-test. Data were presented as mean ± S.D. ($n = 3$ independent samples). $^{*}P < 0.05$. (C) Nanoparticle tracking analysis of EXOs. (D) Transmission electron microscopy image of EXOs. (E) Representative bands of Western blot assay for exosomal markers (CD63) and non-exosomal markers (calnexin and Rab5).

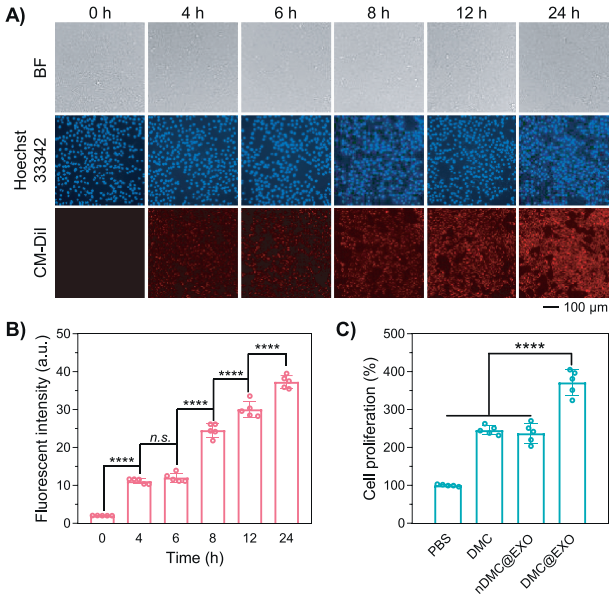

Fig. 3. Enhancement of cell migration verified by transwell assay. (A) Representative fluorescence microscopy images to observe the internalization of CM-DiI-stained EXOs by SMCs. (B) Statistical analysis of fluorescence intensity in (A). (C) Cell counting kit-8 assay to investigate the influence of MSC-EXOs separated by DMCs on the proliferation ability of cells. Statistical analysis was performed using ordinary one-way ANOVA. Data were presented as mean ± S.D. ($n = 5$ independent samples). *n.s.*, $P > 0.05$; $^{****}P < 0.0001$.

results of gel electrophoresis showed that the degradation rate of DMCs was only 10% after 24 h (Fig. S2 in Supporting information), indicating the good stability of DMCs in the serum-containing media.

The influence of polyvalent aptamers in DMCs on separating EXOs was investigated. There was a type of DMCs without aptamers (nDMCs) synthesized with a new template (Template-n in Table S1) as the control. The DMCs and nDMCs were added in the media to separate MSC-EXOs, respectively, in which the EXOs were stained by lipophilic dye (CM-DiI). The capabilities of DMCs and nDMCs on separating EXOs were evaluated by measuring the fluorescence intensity of EXOs in the media before and after separation. As showed in Fig. 2B, the average fluorescence intensity of the EXOs separated by DMCs was significantly higher (1.4 times) than that of the EXOs separated by nDMCs, demonstrating that the specific recognition of polyvalent aptamers to EXOs efficiently enhanced the capability of DMCs on separating EXOs.

The size, morphology and biomarkers of the EXOs in cell culture media were characterized [38]. The size of EXOs was 139.5 ± 1.9 nm measured by nanoparticle tracking analysis (Fig. 2C), and the saucer-shaped morphology of EXOs was observed in transmission electron microscopy image (Fig. 2D), matching the typical structural characteristics of EXOs. The biomarker CD63 of EXOs was detected by western blot assay (Fig. 2E) [36]. The non-exosomal markers, calnexin that was located in endoplasmic reticulum and Rab5 that was located in early endosome and plasma membrane, were detected in cell lysate, with much higher expression than EXOs.

MSC-EXOs have been proven to possess the bioactivities of promoting the proliferation of cells [19]. To prove whether the EXOs separated by the DMC-based strategy remained to promote the proliferation of cells, the cell counting kit-8 (CCK-8) assay was performed to evaluate the proliferation ability of cells after different treatments. Smooth muscle cells (SMCs) were proved to play an important role in the regulation of growth factors and cytokines for wound healing, which was essential for granulation tissue formation [39], and used in the following experiments. Before the experiments, the cytotoxicity of DMCs was evaluated by CCK-8 assay. SMCs were treated with different final concentration of DMCs from 0.125 μg/μL to 2 μg/μL, and the results of CCK-8 assay showed that the viability percentage of SMCs remained higher than 80% compared with the PBS group (Fig. S3 in Supporting information), indicating the low cytotoxicity of DMCs. Consequently, the final concentration of DMCs used in the following cell experiments was 2 μg/μL. Then, to ensure that the EXOs separated by DMCs can produce the promotion effect to cells, the cell internalization of EXOs was investigated. The EXOs were stained by CM-DiI before separation. The analysis results of cell internalization showed that the fluorescence intensities in cells gradually increased in 24 h (Fig. 3A), and the average intensity at 24 h was 3.4 folds of that at 4 h (Fig. 3B), demonstrating the efficient cell internalization of the EXOs separated by DMCs. There were four groups in cell proliferation assay, in which the SMCs were treated with PBS, DMC, nDMC after separating EXOs (nDMC@EXO), and DMC@EXO for 24 h, respectively. After analysis, the average proliferation percentage in DMC@EXO group was significantly higher than that in other groups (Fig. 3C, Fig. S4 and Discussion S1 in Supporting information), 2.7-fold higher than that in PBS group, 0.5-fold higher than that in DMC group, and 0.6-fold higher than that in nDMC@EXO group, respectively. These results indicated that the MSC-EXOs separated by DMCs remained the bioactivities to promote the proliferation of SMCs, and the difference between nDMC@EXO group and DMC@EXO group further demonstrated that the polyvalent aptamers in DMCs can efficiently separate the EXOs from cell culture media.

The migration of cells played important roles in tissue repairing. To investigate the influence of the MSC-EXOs separated by DMCs on the migration ability of SMCs, transwell assay was performed. The SMCs were seeded in the upper chamber with serum-

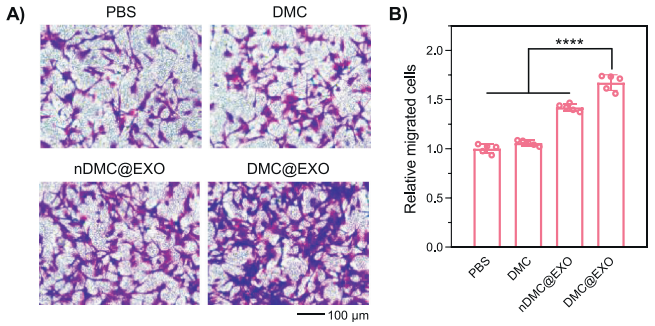

Fig. 4. Enhancement of cell migration verified by transwell assay. (A) Representative microscopy images of the SMCs treated with PBS, DMC, nDMC@EXO and DMC@EXO, respectively. SMCs were treated by crystal violet staining before imaging. (B) Statistics of the migrated cells in the transwell assay. Statistical analysis was performed using ordinary one-way ANOVA. Data were presented as mean ± S.D. ($n = 5$ independent samples). $^{****}P < 0.0001$.

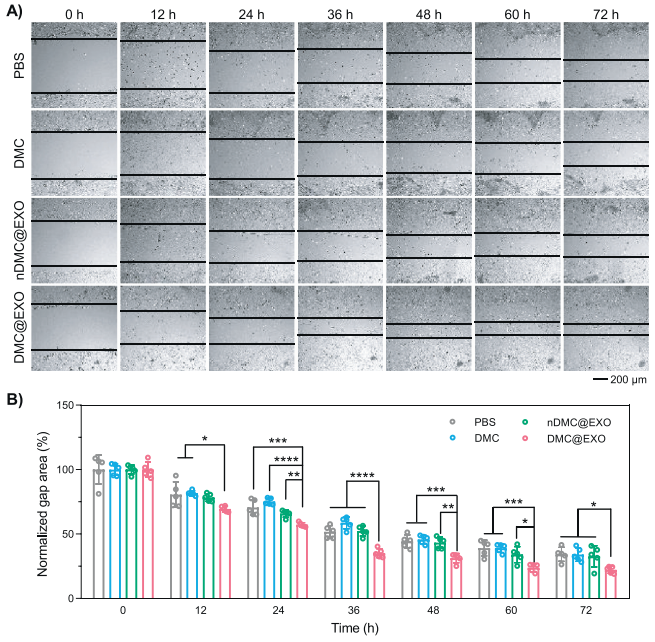

Fig. 5. Enhancement of cell migration verified by scratch assay. (A) Microscopy images of the scratches treated with PBS, DMC, nDMC@EXO and DMC@EXO, respectively. (B) Statistics of gap area in the scratch assay. Statistical analysis was performed using ordinary one-way ANOVA. Data were presented as mean ± S.D. ($n = 5$ independent samples). $^{*}P < 0.05$, $^{**}P < 0.01$, $^{***}P < 0.001$, $^{****}P < 0.0001$.

free culture media, and then treated by PBS, DMC, nDMC@EXO, and DMC@EXO, respectively; the lower chamber was added with culture media containing 10% serum. Due to the concentration difference of nutritional composition, the SMCs migrated to the bottom of upper chamber. After crystal violet staining, the migrated SMCs on the upper chamber were observed by microscopy. As showed in Fig. 4A, there were significant increase of migrated SMCs after DMC@EXO treatment. The statistical results indicated that the migrated SMCs in DMC@EXO group was 0.7-fold higher than that in PBS group, 0.6-fold higher than that in DMC group, and 0.2-fold higher than that in nDMC@EXO group, respectively (Fig. 4B), demonstrating that the MSC-EXOs separated by DMCs efficiently enhanced the migration ability of SMCs.

To further verify the enhancement effect of DMC@EXO on cell migration, scratch assay was performed. The SMCs in a 6-well plate were treated by PBS, DMC, nDMC@EXO, and DMC@EXO, respectively. The scratches were observed by microscopy every 12 h. As showed in Fig. 5A, the scratches in the four groups gradually healed as time. After analysis, there was a significant increase of scratch healing rate in DMC@EXO group compared with other groups (Fig. 5B). At 72 h, the scratch healing rates were 65.8% (PBS), 66.0% (DMC), 67.3% (nDMC@EXO), and 77.8% (DMC@EXO), respectively. These results above demonstrated that the MSC-EXOs separated by DMCs remained the bioactivities to enhance the migration ability of cells, which was essential in wound healing.

Bacterial infection was also an important issue that affected the healing rate of wound. It has been reported that Mg^{2+} played an antibacterial role in regenerative medicine [40,41]. Therefore, the antibacterial function of Mg^{2+}-contained DMCs was investigated, and a type of DMCs containing Ca^{2+} instead of Mg^{2+} (DMC(Ca)) was synthesized as control. The *Escherichia coli* suspension was added into a 96-well plate, and then treated by PBS, DMC(Ca), DMC, and DMC@EXO, respectively. Afterwards, the mixture was added into Luria-Bertani media for extended culture, and the OD_{600} of media was measured after 12 h to monitored the growth of *E. coli*. The results showed that the average OD_{600} in DMC group was significantly lower than that in the groups of PBS and DMC(Ca), which was 69.4% of that in PBS group and 83.8% of that in DMC(Ca) group (Fig. S5 in Supporting information), indicating the efficient inhibition of DMCs on the growth of *E. coli*. These results demonstrated that DMCs had a certain antibacterial function, which was beneficial to wound healing.

To investigate the therapeutic efficiency of DMC@EXO in wound healing, full-thickness wound excision mouse models were established. The animal experiments were approved by Ethics Committee of Tianjin University in compliance with the Animal Management Rules of the Ministry of Health of the People's Republic of China. The results of hemolysis assay showed that the hemolysis percentage after treatment of DMCs was maintained lower than 5%, indicating the good hemocompatibility of DMCs (Fig. S6 in Supporting information). The models were divided into four groups, and treated with PBS, DMC, nDMC@EXO, and DMC@EXO every 3 days, respectively. The situations of wound healing in the four groups were monitored every 2 days (Fig. 6A), until a wound completely healed. The relative wound area at different time points was then calculated according to the photographs. The analysis results showed that there was significant difference on wound healing rate between DMC@EXO group and other groups after the fourth day (Fig. 6B). At the tenth day, the average wound healing rates were 90.8% (PBS), 90.6% (DMC), 95.6% (nDMC@EXO), and 99.6% (DMC@EXO), respectively, showing accelerated wound healing after treatment with the EXOs separated by DMCs.

In summary, we constructed a microscale DNA-based material to separate EXOs from cell culture media for wound healing. The polyaptamers in DMCs were produced *via* RCA, which endowed DMCs with the capability to specifically capture the EXOs in media. The results of cell experiments, including transwell assay and scratch assay, verified that the MSC-derived EXOs separated by DMCs remained the bioactivities to promote the migration of cells, which was the important influencing factor in wound healing. In the full-thickness wound excision mouse model, it was demonstrated that the treatment of the DMCs with EXOs accelerated the wound healing, achieving the complete healing of wound in 10 days.

Compared with other methods of EXO separation, there were three advantages of this DMC-based separation system: (1) The synthesis of separation medium was completed in one-pot, no need for complicated chemical modifications or operations. (2) The separation of EXOs was easily achieved by centrifugation at a low sweep (9705 ×*g*) for 5 min, no need for large precision equipment. (3) Due to the programmability of DNA, more functional DNA units can be introduced into this DMC-based separation system for expanding its biomedical applications such as disease-related biomarker detection [42], achieving the integration of separation

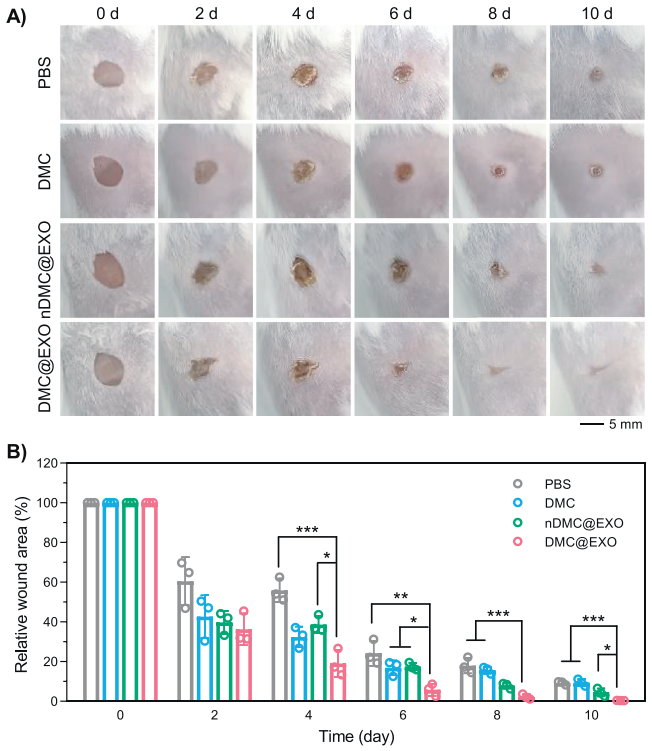

Fig. 6. Promotion of wound healing in full-thickness wound excision mouse models. (A) Pictures of the wounds treated with PBS, DMC, nDMC@EXO and DMC@EXO, respectively. (B) Statistics of wound area in (A). Statistical analysis was performed using ordinary one-way ANOVA. Data were presented as mean ± S.D. ($n = 5$ independent samples). $^{*}P < 0.05$, $^{**}P < 0.01$, $^{***}P < 0.001$.

and application. We envision that this work can provide a new method for EXO separation, and facilitate the development of EXO-based treatments.

Declaration of competing interest

The authors declare that they have no known competing financial interests or personal relationships that could have appeared to influence the work reported in this paper.

Acknowledgments

This work was supported by Tianjin Health Science and Technology Research Project (No. TJWJ2021MS005), National Natural Science Foundation of China (No. 22174097).

Supplementary materials

Supplementary material associated with this article can be found, in the online version, at doi:10.1016/j.cclet.2023.109303.

References

[1] R. Kalluri, V.S. LeBleu, Science 367 (2020) eaau6977.
[2] F. Cocozza, E. Grisard, L. Martin-Jaular, M. Mathieu, C. Thery, Cell 182 (2020) 262.
[3] M. Mathieu, L. Martin-Jaular, G. Lavieu, C. Thery, Nat. Cell Biol. 21 (2019) 9–17.
[4] G. van Niel, D.R.F. Carter, A. Clayton, et al., Nat. Rev. Mol. Cell Biol. 23 (2022) 369–382.
[5] B. Liu, B.W. Lee, K. Nakanishi, et al., Nat. Biomed. Eng. 2 (2018) 293–303.
[6] C. Liu, J. Zhao, F. Tian, et al., Nat. Biomed. Eng. 3 (2019) 183–193.
[7] S. Liu, X. Chen, L. Bao, et al., Nat. Biomed. Eng. 4 (2020) 1063–1075.
[8] W. Zheng, S.M. LaCourse, B. Song, et al., Nat. Biomed. Eng. 6 (2022) 979–991.
[9] Z. Hao, L. Ren, Z. Zhang, et al., Bioact. Mater. 23 (2023) 206–222.
[10] Z. Fang, X. Zhang, H. Huang, J. Wu, Chin. Chem. Lett. 33 (2022) 1693–1704.
[11] S.O. Blacklow, J. Li, B.R. Freedman, et al., Sci. Adv. 5 (2019) eaaw3963.
[12] G. Yao, X. Mo, C. Yin, et al., Sci. Adv. 8 (2022) eabl8379.
[13] G. Theocharidis, H. Yuk, H. Roh, et al., Nat. Biomed. Eng. 6 (2022) 1118–1133.
[14] J. Wu, S. Yao, H. Zhang, et al., Adv. Mater. 33 (2021) 2106175.
[15] P. Xin, S. Han, J. Huang, et al., Chin. Chem. Lett. 34 (2023) 108125.
[16] C. Xian, Z. Zhang, X. You, Y. Fang, J. Wu, Adv. Funct. Mater. 32 (2022) 2202410.
[17] S. Sahoo, D.W. Losordo, Circul. Res. 114 (2014) 333–344.
[18] H. Hashimoto, E.N. Olson, R. Bassel-Duby, Nat. Rev. Cardiol. 15 (2018) 585–600.
[19] Y. Wang, Y. Zhang, T. Li, et al., Adv. Mater. 35 (2023) 2303642.
[20] H. Shao, H. Im, C.M. Castro, et al., Chem. Rev. 118 (2018) 1917–1950.
[21] A. Akbar, F. Malekian, N. Baghban, S.P. Kodam, M. Ullah, Cells 11 (2022) 186.
[22] J. Chen, P. Li, T. Zhang, et al., Front. Bioeng. Biotech. 9 (2022) 811971.
[23] C. Yao, J. Ou, J. Tang, D. Yang, Acc. Chem. Res. 55 (2022) 2043–2054.
[24] C. Liu, J.X. Zhao, F. Tian, et al., J. Am. Chem. Soc. 141 (2019) 3817–3821.
[25] L. Wu, Y. Wang, X. Xu, et al., Chem. Rev. 121 (2021) 12035–12105.
[26] J. Deng, S. Zhao, J. Li, et al., Angew. Chem. Int. Ed. 61 (2022) e202207037.
[27] J. Zhang, W. Li, Y. Qi, et al., Angew. Chem. Int. Ed. 62 (2022) e202214750.
[28] Y. Ouyang, M. Fadeev, P. Zhang, et al., ACS Nano 16 (2022) 18232–18243.
[29] M.M. Ali, F. Li, Z. Zhang, et al., Chem. Soc. Rev. 43 (2014) 3324–3341.
[30] C. Yao, R. Zhang, J. Tang, D. Yang, Nat. Protoc. 16 (2021) 5460–5483.
[31] C. Yao, H. Tang, W.J. Wu, et al., J. Am. Chem. Soc. 142 (2020) 3422–3429.
[32] C. Yao, C. Zhu, J. Tang, et al., J. Am. Chem. Soc. 143 (2021) 19330–19340.
[33] S. Yao, B. Jin, Z. Liu, et al., Adv. Mater. 29 (2017) 1605903.
[34] H. Zhao, J. Lv, F. Li, et al., Biomaterials 268 (2021) 120591.
[35] J. Kowal, G. Arras, M. Colombo, et al., Proc. Natl. Acad. Sci. U. S. A. 113 (2016) E968–E977.
[36] M. Mathieu, N. Nevo, M. Jouve, et al., Nat. Commun. 12 (2021) 4389.
[37] Y. Li, J. Deng, Z. Han, et al., J. Am. Chem. Soc. 143 (2021) 1290–1295.
[38] R. Crescitelli, C. Lasser, J. Lotvall, Nat. Protoc. 16 (2021) 1548–1580.
[39] S. Barrientos, O. Stojadinovic, M.S. Golinko, H. Brem, M. Tomic-Canic, Wound Repair Regen. 16 (2008) 585–601.
[40] T. Ivankovic, H. Turk, J. Hrenovic, et al., J. Hazard. Mater. 458 (2023) 131867.
[41] Q. Li, J. Liu, H. Liu, et al., Bioact. Mater. 29 (2023) 72–84.
[42] J. Tang, X. Jia, Q. Li, et al., Proc. Natl. Acad. Sci. U. S. A. 120 (2023) e2303822120.